Journal of Applied Polymer Science

Characterization and CO_2 Sorption Properties of Poly[methacryloxypropylheptacyclopentyl-T8-silsesquioxane-*co*-3-methacryloxypropyltris(trimethylsiloxy)silane]

Shinji Kanehashi, Yuko Tomita, Hiroshi Kawakita, Shuichi Sato, Tetsuo Miyakoshi, Kazukiyo Nagai
Department of Applied Chemistry, Meiji University, 1-1-1 Higashi-mita, Tama-ku, Kawasaki 214-8571, Japan
Correspondence to: K. Nagai (E-mail: nagai@meiji.ac.jp)

ABSTRACT: Poly[methacryloxypropylheptacyclopentyl-T8-silsesquioxane (MAPOSS)-*co*-3-methacryloxypropyltris(trimethylsiloxy)silane (SiMA)] was synthesized through free radical polymerization. The physical and carbon dioxide (CO_2) sorption properties of the copolymer membranes were investigated in terms of the MAPOSS content. As the MAPOSS content increases, the membrane density increased, suggesting a decrease in the fractional free volume. In addition, the thermal stability was improved with increasing the MAPOSS content. These are because of the polyhedraloligomericilsesquioxane (POSS) units that restrict the high mobility of poly(SiMA) segments. The glass transition temperature, T_g of the copolymers was single T_g based on the differential scanning calorimetry, suggesting that the copolymers were random and not phase separation. Based on the CO_2 sorption measurement, the POSS units play a role in reducing Henry's dissolution by suppressing the mobility of the poly(SiMA) component, while POSS units increase the nonequilibrium excess free volume, which contributes to the Langmuir dissolution. Based on these results, the introduction of MAPOSS unit is one of the effective ways to improved the thermal stability and CO_2 sorption property due to the enhancement of the polymer rigidity. © 2013 Wiley Periodicals, Inc. J. Appl. Polym. Sci. 129: 2036–2045, 2013

KEYWORDS: membranes; separation techniques; radical polymerization; copolymers

Received 6 September 2012; accepted 29 November 2012; published online 7 January 2013
DOI: 10.1002/app.38895

INTRODUCTION

Presently, serious environmental problems such as global warming is caused by the carbon dioxide (CO_2) emission from large fixed sources such as power plants or iron foundries.[1] One of the advantageous separation technologies for CO_2 recovery is membrane-based gas separation. Membrane-based CO_2 separation is performed using the difference between the CO_2 solubility and diffusivity (i.e., solubility selectivity and diffusivity selectivity) and other gases. The high CO_2 solubility is one of the desirable characteristic to more permeable and selectively CO_2. This solubility is foundamentally discussed based on the CO_2 sorption property of polymer membranes.[2]

Polyhedraloligomericilsesquioxane (POSS), small-sized T8 type cubic unit filler, forms eight silicon atoms in a cube in each corner and it is located between the silicon atoms such that oxygen atoms build a bridge. Recently, POSS-containing polymers, such as copolymers[3–13] and composites[3,14–20] have gained much attention because it is expected that the thermal stability,[10,15,16] dielectric,[8] mechanical strength,[13,16] optical,[17] and gas permeation property[9,18–20] are improved by the addition of POSS units. Some reviews on the performance of POSS-containing polymers have also been published.[21,22] However, there are few reports of POSS-containing homopolymer membranes because it is difficult to fabricate the membrane from POSS-containing homopolymers due to the lack of the entanglement affected by the cage-type POSS unit.[1,22–24] Recently, POSS-polyamide self-supporting urtrathin film have fabricated.[25] Additionally, although the CO_2 solubility in the POSS-containing polymers for gas separation is important property, there are few reports for the CO_2 sorption property of POSS-containing composites,[19,20] while there are no studies on the CO_2 sorption property of POSS-containing homopolymer and copolymers. One of the useful approaches in obtaining well-dispersed POSS units in the polymer is random copolymer rather than block to express the property of POSS units.

In this study, the copolymer was synthesized using radical polymerization from cyclopentyle substituted-POSS methacryl polymer and 3-methacryloxypropyltris(trimethylsiloxy)silane(SiMA) as a silicon-containing rubbery polymer to obtain the random copolymer. According to our previous study, poly(SiMA) shows a good gas permeability based on its high free volume.[26] Furthermore, it is expected that the siloxane unit of the SiMA

component has a good compatibility with the POSS unit. The physical and thermal properties of these copolymer membranes were investigated in terms of the POSS content. In addtion, the fundamental CO_2 solubility was also discussed based on the CO_2 sorption property.

EXPERIMENTAL

Chemicals and Synthesis

The monomers used in this study were methacryloxypropylheptacyclopentyl-T8-silsesquioxane (MAPOSS, Gelest, PA) and SiMA (Gelest, PA). SiMA (boiling point = 139°C at 1 Pa), which was liquid at room temperature, was distilled in a vacuum condition. MAPOSS and a,a′-azobis (isobutyronitrile) (AIBN, Junsei Chemical, Tokyo, Japan) as polymerization initiator, which were solid at room temperature, were purified using the recrystallizing method with methanol (Junsei Chemical, Tokyo, Japan), respectively. Polymerization was carried out with AIBN. Toluene (Junsei Chemical, Tokyo, Japan), the polymerization solvent, was distilled in a vacuum and dehydrated with well-dried molecular sieves before use.

Poly(MAPOSS), poly(MAPOSS-*co*-SiMA), and poly(SiMA) were synthesized through free radical polymerization. MAPOSS and SiMA monomers with different composition ratios (100 : 0 mol %; 50 : 50 mol %; 25 : 75 mol %; 10 : 90 mol %; 5 : 95 mol %; 1 : 99 mol %; 0 : 100 mol %) and AIBN were dissolved in toluene at a concentration of 1.0 mol/L and added into the tubes. The tubes were subjected to freeze-dry cycles to remove dissolved oxygen that inhibits polymerization in free radical polymerization. Polymerization was performed at 80°C for 24 h under a high-vacuum condition. The purification was performed using a solution-reprecipitation process with toluene and methanol. The ^{1}H-NMR spectrum of this dried polymer was measured and the aforementioned work was continued until impurities such as monomers, catalysts, and solvents were removed completely.

Membranes Preparation

Poly(MAPOSS), poly(MAPOSS-*co*-SiMA), and poly(SiMA) membranes were prepared by casting a 5 wt % toluene solution of each polymer onto a Teflon Petri dish for 72 h under atmospheric pressure at room temperature. The solvent was allowed to evaporate for 48 h. ^{1}H-NMR analyses confirmed the removal of the residual solvent. The thickness of the membranes used in this study varied between 300 and 400 μm.

Structure Analysis and Characterization

Characterization data were determined in the membrane state in at least three samples to confirm the reproducibility of the experimental results. ^{1}H-NMR and ^{13}C-NMR were performed using JNM-ECA500 (JEOL, Tokyo, Japan). The copolymerization ratio of the copolymer was estimated from the integration on the strength ratio in the NMR spectra. Fourier transforms infrared spectrometry (FT-IR) analysis using the KBr method was carried out with FT/IR-4100 (JASCO, Tokyo, Japan). The measurement conditions were as follows: resolution was 2 cm^{-1}; multiplication number was 32 times; and at 23 ± 1°C.

A solubility test was carried out after 24 h at 23 ± 1°C. The polymers were immersed into methanol, acetone, toluene, hexane, THF, *N*,*N*-dimethylacetamide (DMAc), dimethylsulfoxide (DMSO) (all purchased from Junsei Chemical, Tokyo, Japan), chloroform, and water of 1000 times as much as the solvent as the membrane weight. In addition, the solubility of each solvent was observed for 24 h. The cohesive energy density (CED) was calculated from the Fedors's group contribution method.[27] Other group contribution approaches (such as Small, Hoy, and van Krevenlen) could not be used to compute δ and CED values because the group contribution values for silicon are not available.[28]

Ultraviolet visible (UV–vis) spectrometry analysis in the THF solution was carried out with a Multi spec 1500 UV visible spectrometer (SHIMADZU, Tokyo, Japan) in the wavelength of 190 nm to 800 nm. The multiplication number was 32 times and the measurement temperature was at 23 ± 1°C. Moreover, the constant ε was estimated using Lambert–Beer's equation. The Lambert–Beer law is expressed eq. (1) as follows:

$$A = C \cdot \varepsilon \cdot d \tag{1}$$

where A is the value of the absorbance peak at the maximum absorption wavelength (Abs), ε is the absorption coefficient (wt %/cm), d is the path length of the UV beam in the sample (cm), and C is the concentration of a sample solution (wt %).

The weight average molecular weight M_w, the average molecular weight M_n, and the molecular weight distribution ratio M_w/M_n of the polymers were determined using a gel permeation chromatograph (HLC-8220, Tosoh, Tokyo, Japan) with TSK-gel columns (Super AWM-H) and a detector (RI-8220). The calibration was performed under polystyrene standards at 40°C in the THF solvent at a flow rate of 0.300 mL/min. The inherent viscosity (η_{inh}) of the polymers was measured using a Canon Fensuke viscometer (YOSHIDA SEISAKUSHO, Tokyo, Japan). The viscosity was calculated from 0.5 g/dL of toluene solution at 30°C.

Membrane density (ρ) was measured using the flotation method at 23 ± 1°C with calcium nitrate tetrahydrate (Junsei Chemical Co. Ltd., Tokyo, Japan). The fractional free volume (FFV) of the polymer membranes was determined using the following equation:[28]

$$\mathrm{FFV} = \frac{V - 1.3V_w}{V} \tag{2}$$

where V is the polymer specific volume and V_w is the van der Waals volume calculated by the group contribution method of van Krevelen. The FFV of the copolymer was calculated based on the molar ratio of poly(SiMA) and poly(MAPOSS).[29]

The wide-angle X-ray diffraction (WAXD) measurement was performed on a Rint 1200 X-ray diffractometer (Rigaku, Tokyo, Japan) using a Cu-Kα radiation source. The wavelength of the radiation was 1.54 Å, the maximum intensity in a halo peak was 2θ, and the measurement temperature was 23 ± 1°C. The d-spacing, which presented the mean distance between polymer chains, was calculated from Bragg's conditions.[30]

Thermogravimetric analysis (TGA) of the membranes was carried out using a Pyris 1 TGA Thermo Gravimetric Analyzer (PerkinElmer, Shelton). The polymer sample of about 1.0 mg

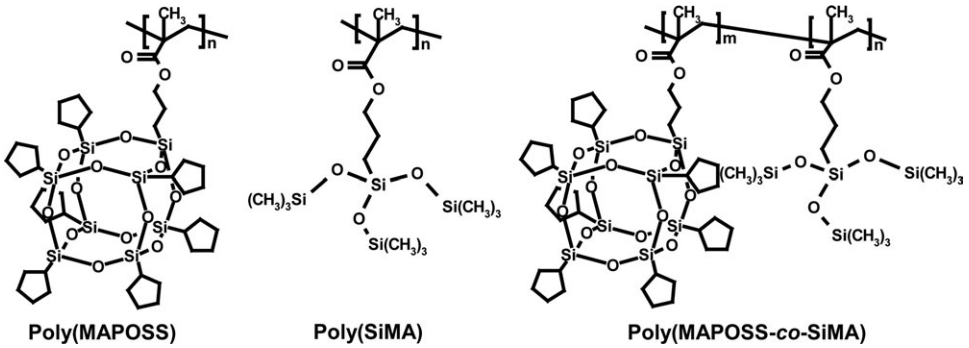

Figure 1. Chemical structures of MAPOSS, poly(MAPOSS-*co*-3-methacryloxypropyl tris(trimethylsiloxy)silane (SiMA)), and poly(SiMA).

was heated from 50 to 900°C in a platinum pan at a heating rate of 10 °C/min under a nitrogen atmosphere at a flow rate of 60 mL/min. The glass transition temperature (T_g) was measured using a Diamond DSC (PerkinElmer, Shelton). Differential scanning calorimeter (DSC) measurements were performed at a range of up to 200°C where pyrolysis did not occur. Heat scan was performed between −100 and 200°C at a heating rate of 20°C/min under a nitrogen atmosphere. The T_g value measured over the second scan was determined as the middle point of the endothermic transition.

The orthoscope observation of the membranes was measured using an Olympus BH-2 Polarization microscope (POM) (Olympus, Tokyo Japan) under a cross-Nicol condition. Polarization images were observed under an additive color at 530 nm with a sensitive color plate. A scanning electron microscope (SEM) in the membranes was performed using a High Resolution Field Emission Scanning Electron microscopy (FE-SEM) (S5200, JEOL, Tokyo Japan).

CO_2 Sorption

Sorption data were determined in the membrane state for at least three samples to confirm the reproducibility of the experimental results. The equilibrium sorption isotherms of pure CO_2 in the poly(MAPOSS), poly(MAPOSS-*co*-SiMA), and poly-(SiMA) membranes were determined using the gravimetric method as a function of pressures up to 40 atm at 35°C using a Cahn-2000 electronic microbalance sorption system placed in a high-pressure chamber with a stepwise increase in pressure.[30–32] The saturated vapor pressure (p_{Sat}) of CO_2 at 35°C is 79.5 atm.[33] The relative pressure (p/p_{Sat}) in the sorption measurements varied over a range of up to 0.5.

RESULTS AND DISCUSSION

Polymer Structure Analysis

The poly(MAPOSS), poly(MAPOSS-*co*-SiMA), and poly(SiMA) were characterized according to their chemical structures by ^{1}H-NMR, ^{13}C-NMR, and FT-IR analyses. The ^{1}H-NMR, ^{13}C-NMR, and FT-IR analyses of these polymers confirmed the chemical structures shown in Figure 1. The polymer properties including the molecular weight, viscosity, and UV–vis property are given in Table I. The molecular weight of all synthesized polymes were over 10,000 g/mol. UV–vis property of all polymers show almost same values of λ_{max} (i.e., 237–240 nm).

The MAPOSS content in each copolymer that was calculated from the integration ratio of ^{1}H-NMR was 100, 50.5, 26.1, 10.4, 6.89, 4.19, and 0 mol %. The copolymerization composition curve of poly(MAPOSS), poly(MAPOSS-*co*-SiMA), and poly(-SiMA) is presented in Figure 2. According to the Fineman and Ross plot, the reactant ratio was $r_1 = 0.58$ for poly(MAPOSS), $r_2 = 0.63$ for poly- (SiMA), and $r_1 \cdot r_2 = 0.37$ for poly(MAPOSS-*co*-SiMA). As r_1 and r_2 were less than 1, we considered that each monomer reacts randomly. Furthermore, although we discussed it later, it is possible to form random copolymers with short block chain lengths because the single T_g was observed in all the copolymers through DSC scanning.

The solubility of poly(MAPOSS) was different from those of poly(MAPOSS-*co*-SiMA) and poly(SiMA). Generally, substituted group in the POSS unit significantly affect the solvent

Table I. Molecular Weight and UV–Vis Property of Poly(MAPOSS-*co*-SiMA)

Polymer	MAPOSS content (mol %)	M_n (g/mol)	M_w (g/mol)	M_w/M_n	η (dL/g)	UV–vis	
						λ_{max} (nm)	ε [1/(wt % cm)]
Poly(MAPOSS)	100	15,000	17,000	1.2	0.03	240	0.20
Poly(MAPOSS-*co*-SiMA)	50.5	144,000	503,000	3.5	0.36	239	0.77
	26.1	163,000	329,000	1.7	0.38	239	0.43
	10.4	153,000	327,000	2.1	0.37	237	0.83
	6.89	119,000	279,000	2.4	0.34	239	0.46
	4.19	64,000	153,000	2.4	0.33	238	0.59
Poly(SiMA)	0	210,000	320,000	1.5	0.58	237	1.36

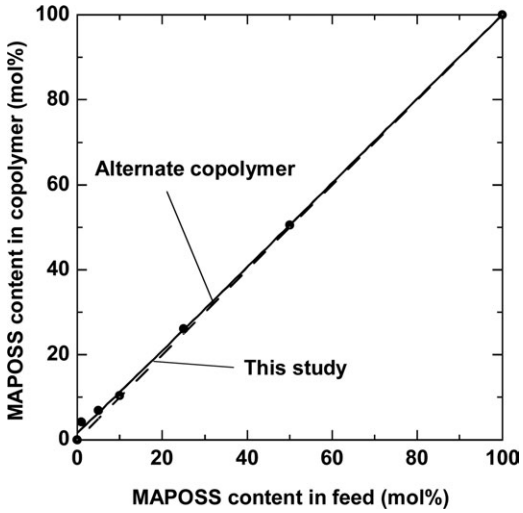

Figure 2. Copolymer composition curve of poly(MAPOSS-*co*-SiMA) based on the Fineman-Ross method. The solid line is the theoretical alternate copolymer and the dotted line is best fit in this study.

solubility.[21,22] Poly(MAPOSS) was partially dissoluble to chloroform, THF, and toluene and insoluble to polar solvents such as methanol, aceton, DMAc, and DMSO. This result of the poly(MAPOSS) was in good agreement with previous literature.[22,24] This solubility could be based on the cyclopentyl group in the POSS unit. Conversely, poly(MAPOSS-*co*-SiMA) and poly(SiMA) dissolved to chloroform, THF, and toluene and insoluble to methanol, aceton, DMAc, and DMSO. Therefore, only the poly(MAPOSS) showed different solubility, and poly(SiMA) component changed the solubility of the poly(MAPOSS-*co*-SiMA).

All the membranes prepared using the casting method were transparent and colorless. The membranes of poly(MAPOSS) and poly(MAPOSS-*co*-SiMA) were very brittle with MAPOSS contents of 50.5 and 26.1 mol %, respectively. Conversely, the membrane with a MAPOSS content of less than 10.4 mol % and poly(SiMA) had good membrane forming abilities. The membrane formation properties decreased with an increasing MAPOSS content. The bulky structure of POSS groups could cause a decrease in the entanglement of polymer chains.[11,22–24]

Membrane Characterization

The physical properties of these membranes are summarized in Table II. The membrane densities of poly(MAPOSS) and poly(SiMA) were 1.221 ± 0.001 and 0.982 ± 0.001 g/cm^3, respectively. The membrane density increased with an increasing MAPOSS content. A simple mixing rule of binary homogenous polymer blends and copolymers estimates the density as:[34]

$$\rho = w_1\rho_1 + w_2\rho_2 \tag{3}$$

where ρ_1 and ρ_2 are the membrane densities (g/cm^3) of components1, 2 in the copolymer, respectively. The w_1 and w_2 are the weight fraction ratios of components1, 2 in the copolymer, respectively. Figure 3 presents the experimental and estimated membrane density of poly(MAPOSS-*co*-SiMA) as a function of MAPOSS content. When the density obeys eq. (3), it increases linearly with increasing MAPOSS content. In the MAPOSS content up to 26.1 mol %, the experimental values are below the estimated ones. For the copolymers with MAPOSS contents of 50.5 and 26.1 mol %, the experimental values are higher than the estimated ones. The introduction of MAPOSS units could provide aggregation of the POSS structures at higher MAPOSS content. The FFV, which presents the amount of space between polymer segments, were 0.086 ± 0.001 and 0.158 ± 0.001 for poly(MAPOSS) and poly(SiMA), respectively. The FFV of poly(MAPOSS) was about 40% lower than that of poly(SiMA). As expected from the membrane density results, the FFV of poly(MAPOSS-*co*-SiMA) decreased with an increasing MAPOSS content. The CED values for poly(MAPOSS) and poly(SiMA) were 402 and 246 MPa, respectively. The larger estimated CED value for poly(MAPOSS) provides a lower FFV and higher membrane density and consequently a more efficient chain packing compared with poly(SiMA). The CED order follows the same order as that of the membrane density, which is the opposite in the case of the FFV.

WAXD Analysis

The wide angle X-ray diffraction (WAXD) patterns of poly(MAPOSS), poly(MAPOSS-*co*-SiMA), and poly(SiMA) are presented in Figure 4. Poly(MAPOSS) was seen at angles $2\theta = 8.3°$ (d = 10.6 Å), 10.6° (d = 8.4 Å), and 18.6° (d = 4.8 Å). These peaks roughly correspond to the 101 and 030 hkl reflections of the rhombohedral unit cell (a = 11.57 Å, $\alpha = 95.5°$) in the POSS

Table II. Physical Properties of Poly(MAPOSS-*co*-SiMA) Membranes

Polymer	MAPOSS content (mol %)	ρ (g/cm^3)	FFV	CED (MPa)	*d*-Spacing (Å)		
					1st	2nd	3rd
Poly(MAPOSS)	100	1.221 ± 0.001	0.086 ± 0.001	402	10.62 ± 0.01	8.36 ± 0.01	4.76 ± 0.01
Poly(MAPOSS-*co*-SiMA)	50.5	1.155 ± 0.001	0.110 ± 0.001	329	10.46 ± 0.01	8.90 ± 0.01	4.74 ± 0.01
	26.1	1.082 ± 0.001	0.128 ± 0.001	305	10.48 ± 0.01	7.93 ± 0.01	4.72 ± 0.01
	10.4	1.025 ± 0.001	0.144 ± 0.001	293	7.39 ± 0.01	4.95 ± 0.01	-
	6.89	1.005 ± 0.001	0.148 ± 0.001	290	7.47 ± 0.01	5.07 ± 0.01	-
	4.19	0.991 ± 0.001	0.152 ± 0.001	288	7.29 ± 0.01	5.07 ± 0.01	-
Poly(SiMA)	0	0.982 ± 0.001	0.158 ± 0.001	246	7.38 ± 0.01	5.10 ± 0.01	-

Applied Polymer SCIENCE

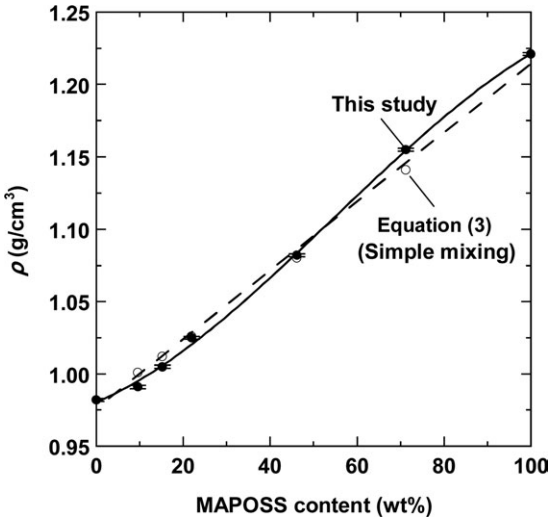

Figure 3. Membrane density of poly(MAPOSS-*co*-SiMA) membranes as a function of the MAPOSS content.

monomer.[11,13] This spectrum suggested that the peaks corresponding to POSS shifted widely between $2\theta = 6°$ and 12°, and the polymer has an amorphous structure. POSS-containing polymers and nanocomposite materials show a crystalline structure.[10,12] Hence, the lack of crystallinity may reflect that the propyl ester linkage is too short to decouple the POSS group from motions of the amorphous backbone. Conversely, there were two broad peaks at $2\theta = 12.0°$ ($d = 7.4$ Å) and $2\theta = 17.4°$ ($d = 5.1$ Å) in poly(SiMA). These two broad halos indicated the distance between polymer segments in a small angle ($2\theta = 12.22°$), whereas that in the large angle ($2\theta = 17.92°$) was attributed to the intermolecular distance between long side chains. Therefore, poly(MAPOSS) and poly(SiMA) were amorphous and there was no ordering of the backbone. All poly(MAPOSS-*co*-SiMA) had amorphous structures based on the WAXD spectra. Interestingly, the peak at $2\theta = 8.3$–$8.4°$, $2\theta = 10.6$–$11.0°$, and $2\theta = 18.6$–$18.8°$ based on the POSS group was observed in the copolymers with an MAPOSS content greater than 26.1 mol %. However, the peak at $2\theta = 8.3$–$8.4°$ and $2\theta = 10.6$–$11.0°$ disappeared and the one at $2\theta = 18.6$–$18.8°$ shifted to 17.5–17.9° in the copolymers with a MAPOSS content less than 10.4 mol %. Therefore, the copolymer can change the effects of poly(MAPOSS) and poly(SiMA) with a MAPOSS content of between 26.1 and 10.4 mol %. The *d*-spacing values of the polymer increased with an increasing MAPOSS content, especially with a MAPOSS content greater than 26.1 mol %.

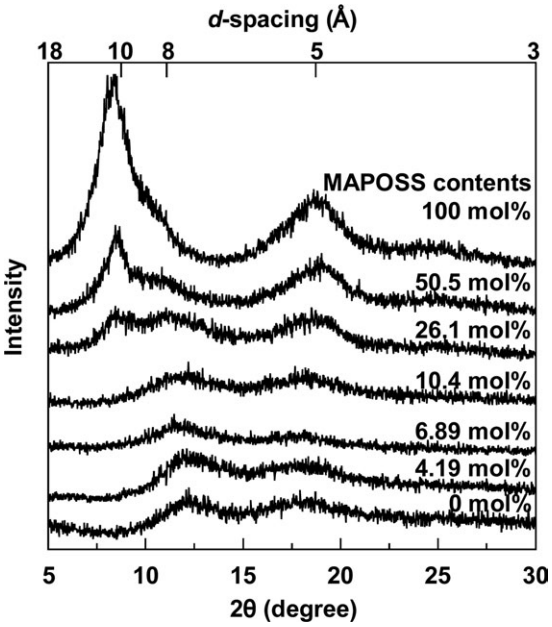

Figure 4. Wide angle X-ray diffraction (WAXD) profile of poly(MAPOSS-*co*-SiMA) membranes.

Thermal Property

The TGA curves of poly(MAPOSS), poly(MAPOSS-*co*-SiMA), and poly(SiMA) are presented in Figure 5. The thermal properties of poly(MAPOSS), poly(MAPOSS-*co*-SiMA), and poly(SiMA) are shown in Table III. The decomposition temperatures of poly(MAPOSS) and poly(SiMA) were 387 ± 7°C and 320 ± 2°C, respectively. The decomposition temperature of the copolymers was largely increased with an increasing MAPOSS content of over 50.5 mol %. Therefore, the POSS group in the copolymers restricted the mobility of the SiMA component. The residual weight of poly(MAPOSS-*co*-SiMA) at 900°C was increased with an increasing MAPOSS content. These values correspond to the POSS groups in the copolymers. The residual weight of poly(MAPOSS) was higher than that in theory compared with that of copolymers with a MAPOSS content below 50.5 mol %, which were lower than that in theory. This is because the random distribution of POSS groups can be affected.

The glass transition temperatures (T_g) of poly(MAPOSS) and poly(SiMA) were 151 ± 6°C and −6 ± 1°C, respectively. The T_g of poly(MAPOSS-*co*-SiMA) was observed in a single value, suggesting that the random copolymers were synthesized. An increase in T_g was observed as the MAPOSS content was increased. Hence, the MAPOSS content can restrict the mobility of flexible SiMA structures. According to the DSC measurements, the copolymers with a MAPOSS content of over 26.1 mol % were in glassy states and those with a MAPOSS content

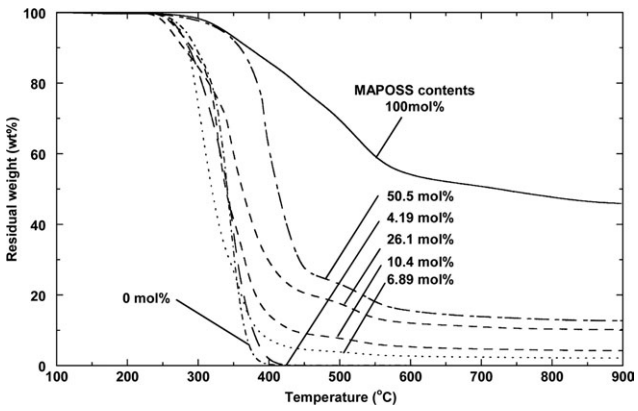

Figure 5. Thermo gravimetric analysis (TGA) curves of poly(MAPOSS-*co*-SiMA) membranes.

Table III. Thermal Properties of Poly(MAPOSS-*co*-SiMA) Membranes

Polymer	MAPOSS content (mol %)	T_5 (°C)	T_{10} (°C)	T_d (°C)	W_R (wt %)	T_g (°C)	ΔC_p [J/(g·°C)]
Poly(MAPOSS)	100	336 ± 5	372 ± 1	387 ± 7	44.3 ± 2.8	151 ± 6	0.512 ± 0.289
Poly(MAPOSS-*co*-SiMA)	50.5	332 ± 3	359 ± 3	382 ± 6	13.7 ± 1.1	73.1 ± 3.1	0.051 ± 0.005
	26.1	261 ± 1	280 ± 3	315 ± 4	10.6 ± 0.6	45.2 ± 4.3	0.092 ± 0.012
	10.4	272 ± 3	291 ± 6	308 ± 2	3.8 ± 0.6	15.2 ± 4.9	0.079 ± 0.021
	6.89	275 ± 3	285 ± 7	286 ± 4	1.9 ± 0.4	9.6 ± 7.3	0.053 ± 0.011
	4.19	273 ± 6	287 ± 5	309 ± 1	0.0 ± 0.1	5.0 ± 2.3	0.105 ± 0.092
Poly(SiMA)	0	281 ± 7	297 ± 3	320 ± 2	0.0 ± 0.1	−6.3 ± 1.3	0.103 ± 0.088

of less than 10.4 mol % were in rubbery states. This content between 26.1 and 10.4 mol % correspond to the result of the properties that were change based on the WAXD analysis.

T_g of polymer can be estimated from two predictive equations: the simple mixing rule of mixtures in eq. (4) and the Fox equation in eq. (5).[34,35]

$$T_g = w_1 T_{g1} + w_2 T_{g2} \tag{4}$$

$$\frac{1}{T_g} = \frac{w_1}{T_{g1}} + \frac{w_2}{T_{g2}} \tag{5}$$

where T_{g1} and T_{g2} are T_g of components 1, 2, respectively. The w_1 and w_2 are the weight fraction ratios of components1, 2 in the copolymer, respectively. The Fox relation is considered an ideal volume additivity equation for the T_g of compatible copolymers or polymer blends. Figure 6 indicates that the poly-(MAPOSS-*co*-SiMA) obeyed the predictions of Fox. The deviation from the Fox equation was observed at high concentration of MAPOSS. The negative deviation indicates that the interactions of copolymer or polymer blends are lower due to the less compatibility. Therefore, the deviation from the Fox at high content of MAPOSS could be related to the aggregation of MAPOSS units, leading to looser compatibility.

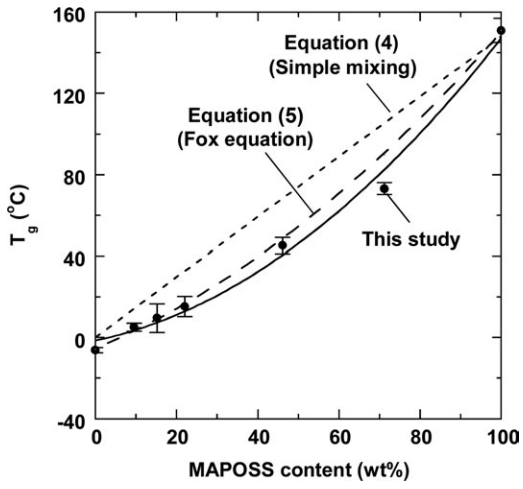

Figure 6. Glass transition temperature (T_g) of poly(MAPOSS-*co*-SiMA) membranes as a function of its MAPOSS content.

POM and SEM images of poly(MAPOSS), poly(MAPOSS-*co*-SiMA), and poly(SiMA) membranes are presented in Figure 7. There was no obvious color contrast in the POM images, suggesting that all the polymer membranes had a complete amorphous structure as expected from the WAXD analysis, regardless of the presence of the POSS unit. Conversely, SEM images also showed the somewhat rough structure, indicative of nonuniform structure in the poly(MAPOSS) material, with the size of

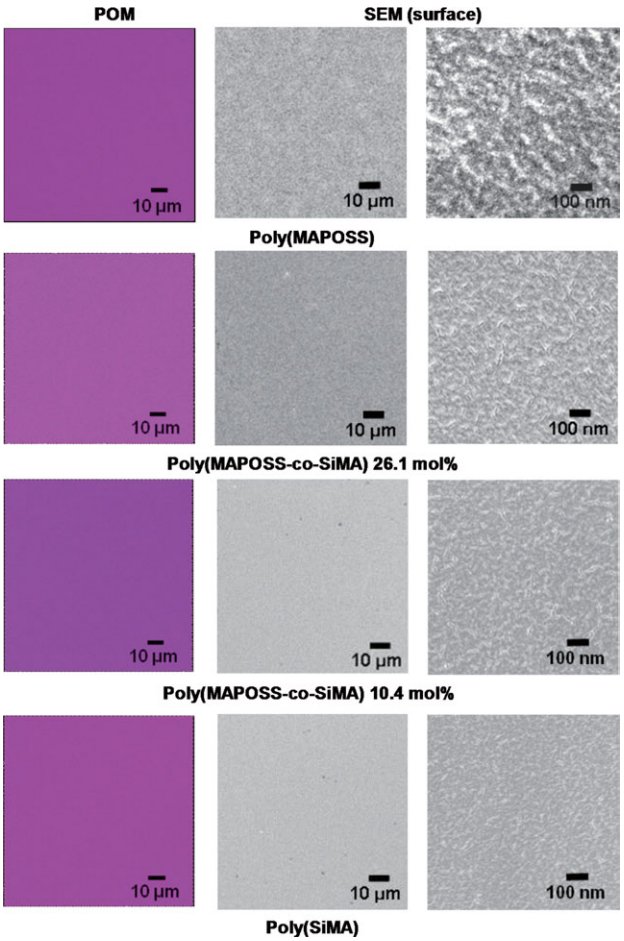

Figure 7. POM and SEM images of the membrane surface in poly(MAPOSS-*co*-SiMA) membranes. [Color figure can be viewed in the online issue, which is available at wileyonlinelibrary.com.]

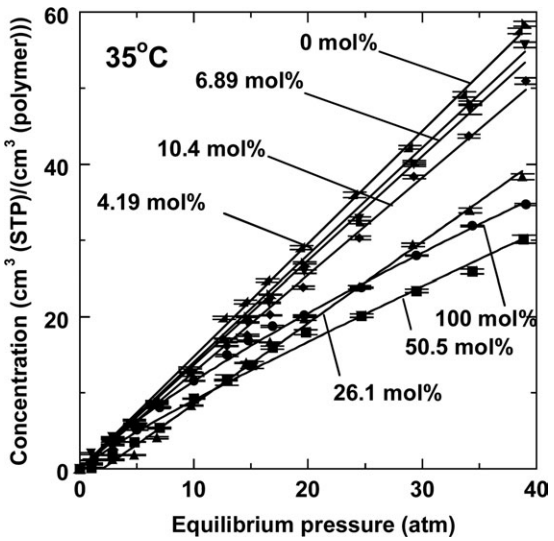

Figure 8. Sorption isotherms for CO_2 at 35°C in poly(MAPOSS-*co*-SiMA) membranes. 100 mol % (●), 50.5 mol % (■), 26.1 mol % (▲), 10.4 mol % (◆), 6.89 mol % (▼), 4.19 mol % (◣), and 0 mol % (◢) of MAPOSS content.

the surface features decreasing as the MAPOSS content is reduced. This result suggests that the aggregation of the POSS structures when present in high concentrations.

CO_2 Sorption

CO_2 sorption isotherms in poly(MAPOSS), poly(MAPOSS-*co*-SiMA), and poly(SiMA) membranes at 35°C are presented in Figure 8. The CO_2 uptake is higher in poly(SiMA) than in poly(MAPOSS). The order of CO_2 concentration decreased with increasing POSS content due to the decrease in the high free volume based on the SiMA component. Only the CO_2 uptake of poly(MAPOSS-*co*-SiMA) (50.5mol %) was below that of poly(MAPOSS). The aggregation of MAPOSS units could be related to the decrease in the sorption property at highly MAPOSS content. As expected in amorphous, rubbery polymers, the CO_2 sorption isotherms in poly(SiMA) and poly(MAPOSS-*co*-SiMA) (4.19, 6.89, and 10.4 mol %) membranes increase in a linear manner to the pressure axis. This behavior is specific to Henry's law dissolution as the following equation:[2]

$$C = C_D = k_D p \tag{6}$$

where C is the concentration [cm^3 (STP)/(cm^3 (polymer))], p is the equilibrium pressure (atm), k_D represents Henry's law constant, and C_D is the gas concentration in Henry's law sites. Conversely, the CO_2 sorption isotherms in poly(MAPOSS) and poly(MAPOSS-*co*-SiMA) (50.5 and 26.1 mol %) membranes are concave to the pressure axis. This behavior is specific to the dual-mode sorption as the following equation:[2]

$$C = C_D + C_H = k_D p + \frac{C'_H bp}{1 + bp} \tag{7}$$

where C_H is the gas concentration in the Langmuir-type hole filling sites, b is the Langmuir affinity parameter (1/atm), and C'_H is the Langmuir capacity parameter [cm^3 (STP) /(cm^3(polymer))]. The sorption coefficient of the penetrant dissolved in the equilibrium regions of the polymer matrix is k_D, b characterizes the tendency of a penetrant to sorb into a Langmuir site, and C'_H is a measure of the maximum sorption capacity of the Langmuir domains. The C'_H value is related to the nonequilibrium excess free volume in a glassy polymer and can be expressed as follows:[2,32]

$$C'_H = \left(\frac{V_g - V_l}{V_g}\right)\rho^* \tag{8}$$

where V_g and V_l are the polymer specific volumes (cm^3/g) in the glassy and hypothetical rubbery states, respectively, and ρ^* is the molar density (mol/cm^3) of the penetrant as it exists in the Langmuir sites. The ρ^* value of carbon dioxide at 35°C is 0.0182 mol/cm^3.[36] Dual-mode parameters obtained from a nonlinear least square regression analysis of the carbon dioxide sorption data in Figure 8 are summarized in Table IV. As expected from Figure 8, the k_D value decreased with an increasing MAPOSS content. The k_D value of poly(SiMA) is about two times larger than that of poly(MAPOSS). This is because poly(SiMA) has a higher free volume based on the flexible bulky trimethylsilyl group. The order of the k_D value follows the same order of that of the FFV value. The C'_H value decreased and the b value in glassy polymers increased with a decreasing MAPOSS content. The C'_H/ρ^* value is 0.036 for poly(MAPOSS), 0.015 for 50.5 mol %, and 0.002 for 26.1 mol %.

The parameters k_D, C'_H, and b values of the polymer membranes at 35°C as a function of the MAPOSS content in each polymer are shown in Figure 9. These parameters exhibit good

Table IV. Dual-Mode Sorption Parameters for CO_2 in Poly(MAPOSS-*co*-SiMA) Membranes

Polymer	MAPOSS content (mol %)	State at 35°C	k_D [cm^3(STP)/(cm^3(polymer) atm)]	C'_H [cm^3(STP)/(cm^3(polymer))]	C'_H/ρ^*	b (1/atm)
Poly(MAPOSS)	100	Glassy	0.63 ± 0.01	14.7 ± 0.4	0.036	0.087 ± 0.005
Poly(MAPOSS-*co*-SiMA)	50.5	Glassy	0.69 ± 0.02	6.15 ± 1.25	0.015	0.104 ± 0.019
	26.1	Glassy	0.96 ± 0.02	0.90 ± 0.80	0.002	0.160 ± 0.018
	10.4	Rubbery	1.33 ± 0.01	0.00	0.00	0.00
	6.89	Rubbery	1.42 ± 0.01	0.00	0.00	0.00
	4.19	Rubbery	1.42 ± 0.01	0.00	0.00	0.00
Poly(SiMA)	0	Rubbery	1.48 ± 0.01	0.00	0.00	0.00

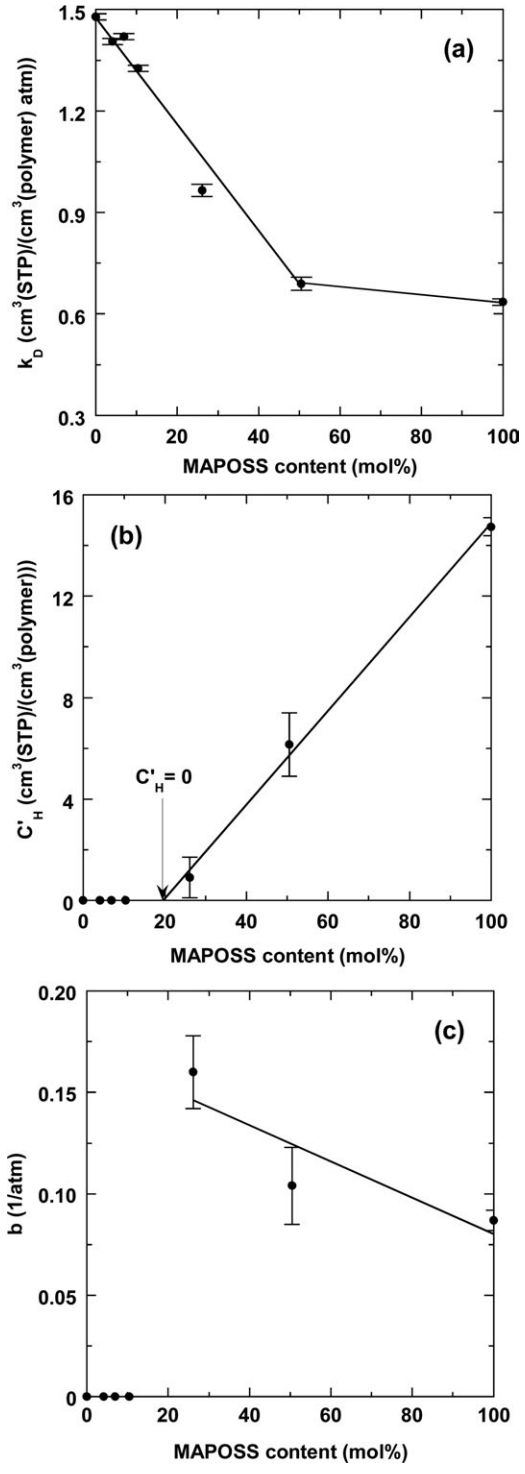

Figure 9. Dual mode sorption parameters of poly(MAPOSS-*co*-SiMA) membranes as a function of its MAPOSS content. (a) Henry's law constant (k_D), (b) Langmuir capacity constant (C'_H), and (c) hole affinity constant (b).

relationships with the MAPOSS content. The k_D value decreased linearly between a MAPOSS content of 0–50.5 mol %. Then, the value of 50.5 mol % and poly(MAPOSS) was almost same. Therefore, the aggregation of POSS units in the copolymers with a MAPOSS content of over 50.5 mol % affects the flexible poly(SiMA) and there was a significant decrease in the CO_2 dissolution into Henry's region. The C'_H value of the glassy polymer membranes at 35°C increased linearly with an increasing MAPOSS content, which followed the trend in that of polymer T_g. The C'_H value of the rubbery polymers at 35°C is zero, indicating that the rubbery polymer does not contain the nonequilibrium excess free volume in the polymer. According to our previous study, there is a relationship between the C'_H value and polymer T_g.[2] Based on this relationship, the MAPOSS content at $C'_H = 0$ estimated from the extrapolation in Figure 9(b) was about 20 mol %. Hence, T_g can be estimated at about 35°C, which is the experimental temperature. The b value of the glassy polymer membranes at 35°C decreased linearly with an increasing MAPOSS content, which was the same trend in FFV. The b value represents the ratio between the aggregation kinetics of gas molecules into polymer membranes based on the kinetics of gas molecules and desorption of sorbed gas molecules from the polymer membranes. Therefore, the POSS unit can play a role in increasing the interaction with CO_2 molecules.

The solubility S [cm^3 (STP)/(cm^3 (polymer) atm)] can be written using the dual-mode sorption parameters as follows:[2,30,32]

$$S = \frac{C}{p} = S_D + S_H = k_D + \frac{C'_H b}{1 + bp} \tag{9}$$

where S_D and S_H are the solubilities based on Henry's law sites [cm^3 (STP)/(cm^3(polymer) atm)] and Langmuir-type hole sites (cm^3 (STP)/(cm^3 (polymer) atm)), respectively. The infinite dilution solubility S_0 [cm^3 (STP)/(cm^3 (polymer) atm)] is given as follows:[2,32]

$$S_0 = \lim_{p \to 0} \left(\frac{C}{p} \right) \approx S_{D0} + S_{H0} = k_D + C'_H b \tag{10}$$

where S_{D0} is the infinite dilution solubility in Henry's law sites [cm^3 (STP)/(cm^3(polymer) atm)] and S_{H0} is the infinite

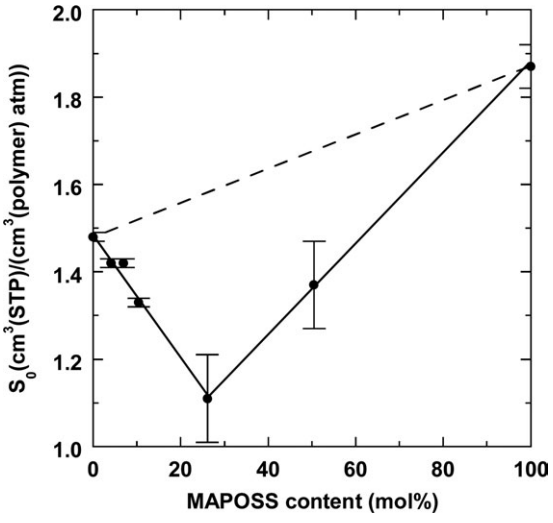

Figure 10. Infinite dilution carbon dioxide solubility at 35°C in poly(MAPOSS-*co*-SiMA) membranes.

Applied Polymer SCIENCE

dilution solubility in Langmuir-type sites [cm^3 (STP)/(cm^3-(polymer) atm)]. The saturation pressure p_0 of carbon dioxide at 35°C is 79.5 atm.[33] Therefore, the relative pressure p/p_0 of CO_2 at 40 atm is 0.5. The S_0 and S_{H0} values were estimated from eqs. (9) and (10) using the dual-mode sorption parameters in Table IV. The S_0 value is 26% larger for poly(MAPOSS) relative to poly(SiMA). The S_0 order is poly(MAPOSS) > poly(SiMA) > 6.89 > 4.19 > 50.5 > 10.4 > 26.1 mol %, which did not follow the MAPOSS content as presented in Figure 10. The solubility at an infinite dilution was affected by the balance of the POSS unit and SiMA unit, which is flexible and has a high free volume. Interestingly, the solubility at an infinite dilution of poly(MAPOSS) is highest value among these copolymers, suggesting that the CO_2 molecule preferes to dissolve the poly(MAPOSS) than the flexible poly(SiMA) which has high free volume at infinite dilution. Hence, we found that the CO_2 solubility of the POSS unit based on the Langmuir dissolution is higher than that of the flexible trimethylsiloxy group based on the Henry's dissolution at infinite dilution.

The proportion of the excess free volume fraction to the total solubility (C'_H/ρ^*)/FFV as a function of T_g −35°C is presented in Figure 11(a) to discuss the effect of POSS units in the Langmuir dissolution. As T_g increased, (C'_H/ρ^*)/FFV linearly increased. This result was similar to other glassy polymers.[2] Hence, the POSS unit increased the excess free volume in the polymers. The linear retionship was also observed between (C'_H/ρ^*)/FFV and the ratio of the Langmuir-type contribution in S_0 (i.e., S_{H0}/S_0) as presented in Figure 11(b). The S_{H0}/S_0 increased from 0 to 0.55 with an increasing MAPOSS content. Therefore, the ratio of the excess free volume depends on the Langmuir-type contribution fraction at infinite dilution in this study.

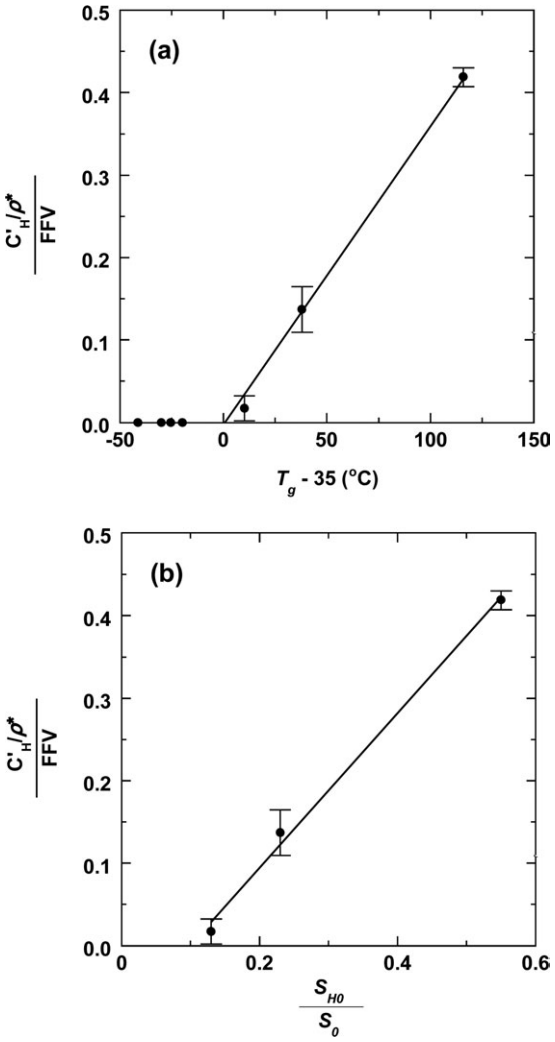

Figure 11. The nonequilibrium excess free volume fraction in the total free volume as a fuction of polymer glass transition temperature (a) and the Langmuir-type contribution solubility at infinite dilution (b) in poly(MAPOSS-*co*-SiMA) membranes.

CONCLUSION

A novel random copolymer that consists of MAPOSS and 3-methacryloxy propyltris(trimethylsiloxy)silane (SiMA) was synthesized through free radical polymerization. The physical and CO_2 sorption properties of the copolymer membranes were investigated in terms of its MAPOSS content. According to the Fineman–Ross method, the synthesized polymers were random copolymers. In addition, the polymer glass transition temperature was single based on the differential scanning calorimetry, suggesting that the polymers were random and not block or phase separation. The membrane density increased, while the thermal stability improved with an increasing MAPOSS content due to the suppression of the mobility of poly(SiMA) segments by POSS units. X-ray diffraction patterns of all polymer membranes show an amorphous structure regardless of the MAPOSS content. The CO_2 sorption isotherms in poly(MAPOSS) and poly(MAPOSS-*co*-SiMA) (50.5 and 26.1 mol %) membranes at 35°C are concave to the pressure axis, indicating a characteristic of the dual-mode sorption model. Meanwhile, those in poly(SiMA) and poly(MAPOSS-*co*-SiMA) (10.4, 6.89, and 4.19 mol %) show a linear increase to the pressure axis, indicating a characteristic of Henry's law of dissolution. The C'_H value of glassy membranes at 35°C increased, while the k_D and b values decreased with an increasing MAPOSS content. Based on these results, the POSS units play a role in reducing Henry's dissolution because of the suppression of the high mobility of poly(SiMA) segments, while POSS units increase the nonequilibrium excess free volume, which contribute to the Langmuir dissolution. Based on these results, the introduction of MAPOSS unit is one of the effective ways to improved the thermal stability and CO_2 sorption property due to the enhancement of the polymer rigidity.

ACKNOWLEDGMENTS

This research was partially supported by a Grant-in-aid for Scientific Research C (24560862) and Grant-in-Aid for JSPS Fellows from the Ministry of Education, Culture, Sports, Science and Technology, Japan, the Japanese Society of the Promotion of Science and Research Project Grant B (3) from the Institute of Science and Technology, Meiji University, Japan.

REFERENCES

1. Freeman, B. D.; Yampolskii, Y., Membrane Gas Separation; Wiley; West Sussex, **2010**.
2. Kanehashi, S.; Nagai, K.; *J. Membr. Sci.* **2005**, *253*, 117.
3. Li, G. Z.; Cho, H.; Wang, L.; Toghiani, H.; Pittman, C. U., Jr. *J. Polym. Sci. Part A: Polym. Chem.* **2005**, *43*, 355.
4. Schwab, J. J.; Lichtenhan, J. D. *Appl. Organometal. Chem.* **1998**, *12*, 707.
5. Zhang, W. H.; Fu, B. X.; Seo, Y.; Schrag, E.; Hsiao, B.; Mather, P. T.; Yang, N. L.; Xu, D. Y.; Ade, H.; Rafailovich, M.; Sokolov, J. *Macromolecules* **2002**, *35*, 8029.
6. Hirai, T.; Leolukman, M.; Jin, S.; Goseki, R.; Ishida, Y.; Kakimoto, M. A.; Hayakawa, T.; Ree, M.; Gopalan, P. *Macromolecules* **2009**, *42*, 8835.
7. Hirai, T.; Leolukman, M.; Liu, C. C.; Han, E.; Kim, Y. J.; Ishida, Y.; Hayakawa, T.; Kakimoto, M.; Nealey, P. F.; Gopalan, P. *Adv. Mater.* **2009**, *21*, 4334.
8. Leu, C. M.; Chang, Y. T.; Wei, K. H. *Macromolecules* **2003**, *36*, 9122.
9. Rios-Dominguez, H.; Ruiz-Trevino, F. A.; Contreras-Reyes, R.; Gonzalez-Montiel, A. *J. Membr. Sci.* **2006**, *271*, 94.
10. Romo-Uribe, A.; Mather, P. T.; Haddad, T. S.; Lichtenhan, J. D. *J. Polym. Sci. Part B: Polym. Phys.* **1998**, *36*, 1857.
11. Pyun, J.; Matyjaszewski, K.; Wu, J.; Kim, G.-M.; Chun, S. B.; Mather, P. T. *Polymer* **2003**, *44*, 2739.
12. Zheng, L.; Waddon, A. J.; Farris, R. J.; Coughlin, E. B. *Macromolecules* **2002**, *35*, 2375.
13. Fu, B. X.; Hsiao, B. S.; Pagola, S.; Stephens, P.; White, H.; Rafailovich, M.; Sokolov, J.; Mather, P. T.; Jeon, H. G.; Phillips, S.; Lichtenhan, J.; Schwab, J. *Polymer* **2001**, *42*, 599.
14. Dorigato, A.; Pegoretti, A.; Migliaresi, C. *J. Appl. Polym. Sci.* **2009**, *114*, 2270.
15. Zheng, L.; Farris, R. J.; Coughlin, E. B. *Macromolecules* **2001**, *34*, 8034.
16. Tanaka, K.; Adachi, S.; Chujo, Y. *J. Polym. Sci. Part A: Polym. Chem.* **2009**, *47*, 5690.
17. Tanaka, K.; Adachi, S.; Chujo, Y. *J. Polym. Sci. Part A: Polym. Chem.* **2010**, *48*, 5712.
18. Dasgupta, B.; Sen, S. K.; Banerjee, S. *Mater. Sci. Eng. B* **2010**, *168*, 30.
19. Hao, N.; Böhning, M.; Schönhals, A. *Macromolecules* **2010**, *43*, 9417.
20. Iyer, P.; Iyer, G.; Coleman, M. *J. Membr. Sci.* **2010**, *358*, 26.
21. Kuo, S.-W.; Chang, F.-C. *Prog. Polym. Sci.* **2011**, *36*, 1649.
22. Li, G. Z.; Wang, L.; Ni, H.; Pittman, C. U., Jr. *J. Inorg. Organomet. Polym.* **2002**, *11*, 123.
23. Pyun, J.; Matyjaszewski, K. *Macromolecules* **2000**, *33*, 217.
24. Lichtenhan, J. D. O., Yoshiko A.; Carr, Michael J. *Macromolecules* **1995**, *28*, 3.
25. Dalwani, M.; Zheng, J.; Hempenius, M.; Raaijmakers, M. J. T.; Doherty, C. M.; Hill, A. J.; Wessling, M.; Benes, N. E. *J. Mater. Chem.* **2012**, *22*, 14835.
26. Nakagawa, T.; Nagashima, S.; Higuchi, A. *Desalination* **1993**, *90*, 183.
27. Fedors, R. F. *Polym. Eng. Sci.* **1974**, *14*, 147.
28. Krevelen, D. W. V., Properties of Polymers 3rd ed.; Elsevier: Amsterdam, **1990**.
29. Yeong, Y. F.; Wang, H.; Pallathadka Pramoda, K.; Chung, T.-S. *J. Membr. Sci.* **2012**, *397–398*, 51.
30. Kanehashi, S.; Nakagawa, T.; Nagai, K.; Duthie, X.; Kentish, S.; Stevens, G. *J. Membr. Sci.* **2007**, *298*, 147.
31. Nakagawa, T.; Nishimura, T.; Higuchi, A. *J. Membr. Sci.* **2002**, *206*, 149.
32. Nagai, K.; Kanehashi, S.; Tabei, S.; Nakagawa, T. *J. Membr. Sci.* **2005**, *251*, 101.
33. Poling, B. E.; Prausnitz, J. M.; O'Connell, J. P. The Properties of Gases and Liquids, 5th ed.; McGraw-Hill: New York, **2000**.
34. Akiba, C.; Watanabe, K.; Nagai, K.; Hirata, Y.; Nguyen, Q. T. *J. Appl. Polym. Sci.* **2006**, *100*, 1113.
35. Fox, T. G. *Bull. Am. Phys. Soc.* **1956**, *1*, 123.
36. Prausnitz, J. M.; Shair, F. H. *AIChE J.* **1961**, *7*, 682.